

Article



Magnetic and Magnetoelectric Properties of Aurivillius Threeand Four-Layered Intergrowth Ceramics

Vadla Veenachary ¹, E. V. Ramana ², S. Narendrababu ¹, Venkata Sreenivas Puli ^{3,6,*}, Adiraj Srinivas ⁴, Gapalan Srinivasan ⁵, Sujoy Saha ⁵, G. Prasad ¹ and N. V. Prasad ^{1,*}

- Materials Research Laboratory, Department of Physics, Osmania University, Hyderabad, 500 013 In-dia;veenachary1@gmail.com_(V.V.);narendraphysics@gmail.com (S.N.B.);
- ² 45433, USAal3N-Aveiro, Department of Physics, University of Aveiro, Aveiro-3810 193, Portugal; raman.venkata@ua.pt
- ³ Smart Nanomaterials Solutions, Orlando, FL, 32707, USA;pvsri123@gmail.com
- 4 Advanced Magnetics Group, Defence Metallurgical Research Laboratory, Hyderabad, 500 058 India;adirajs@gmail.com
- ⁵ Physics Department, Oakland University, Rochester, Michigan, USA;srinivas@oakland.edu
- ⁶ National Research Council, Washington, DC 20001, USA
- * Correspondence: nvp1969@rediffmail.com, pvsri123@gmai.com

Abstract: In this work, we have prepared intergrowth of multiferroic compounds namely Bi₄RTi₃Fe_{0.7}Co_{0.3}O₁₅ - Bi₃RTi₂Fe_{0.7}Co_{0.3}O₁₂₋₆ (BRTFCO₁₅-BRTFCO₁₂) (rare earth (R) =Dy, Sm, La) by solid-state reaction method. From the X-ray diffraction Rietveld refinement, the structure of the intergrowths was found to be orthorhombic in which satisfactory fittings establish the existence of three-layered (space group: b 2 c b) and four-layered compounds (space group: A2₁am). Analysis of magnetic measurements confirmed a larger magnetization for the Sm-modified intergrowth compound (BSTFCO₁₅-BSTFCO₁₂) compared to Dy- and La-doped ones. The emergence of higher magnetic properties can be due to distortion in the unit cell when some Bi³⁺ ions are replaced with the Sm³⁺, bonding of Fe³⁺-O-Co³⁺ as well as a possible mixture of Fe_xCo_y - type nanoparticles that are formed generally in the synthesis of intergrowths. The changes in the magnetic state of the Aurivillius intergrowths have been reflected in the magnetoelectric (ME) coupling: higher ME coefficient (~ 30 mV/Cm-Oe) at lower magnetic fields and is constant up to 3 kOe. The results were corroborated by Raman spectroscopy and variation of temperature with magnetization data. The results revealed that the RE-modified intergrowth route is an effective preparative method for higher-layer Aurivillius multiferroic ceramics.

Keywords: Magnetoelectric; Multiferroic; Aurivillius Intergrowth compounds; Magnetic studies; Raman spectroscopy;

Citation:Veenachary, V.; Ramana, E,V. Narendrababu, S.; Puli, V.S.; Srinivas, A.; Srinivasan, G.; Saha, S.;

Prasad, G.; Prasad, N.V.;Magnetic and Magnetoelectric Properties of Aurivillius Three- and Four-Layered Intergrowth Ceramics. *Crystals* **2023**, 13, x. https://doi.org/10.3390/xxxxx

Academic Editor: Claudio Cazorla

Received: 20 February 2023 Revised: 26 February 2023 Accepted: 27 February 2023 Published: date



Copyright:© 2023by the authors. Submitted for possible open access publication under the terms and conditions of the Creative Commons Attribution (CC BY) license (https://creativecommons.org/license s/by/4.0/).

1. Introduction

Aurivillius oxides with Bismuth layer structure and the chemical formula: (An-1BnO3n+1)²- (Bi2O2)²+ are known to possess excellent magnetoelectric properties and stable ferroelectric polarization [1,2]. Here A- stands for mono-, di-, or trivalent cation or a mixture of them at a 12-coordinate site. The term B- represents tri-, tetra-, or pentavalent cations at the 6- coordinate site. The term 'n' indicates the number of layer compounds or perovskite units [1]. The structure of the compounds consists of alternative perovskite blocks of (Am-1BmO3m+1)²- and are interleaved with the bismuth oxide layers (Bi2O2)²+ along with the pseudo-tetragonal c-axis. The said above compounds are found to be interesting from the scientific and technological point of view like in piezoelectric devices, memory devices, pyro sensors, and magnetoelectric sensors [2–5]. Bi4Ti3O12 compound is a three-layered compound having a high transition temperature (Tc~ 675°C) and high electrical leakage currents. To reduce its limitation, rare earth elements were substituted for Bi³+

ions for fine-tuning the physical properties. In addition, Sr²⁺ modified bismuth-based four-layered compounds were found to be phase-stable and the Sr-O bond suppresses the bismuth evaporation during the sintering stage. The intergrowth compounds of Sr modified 3-layered and five-layered were found to be interesting owing to the fact of their high dielectric properties [6,7]. Alternatively, many Aurivillius phase compounds have shown multiferroic properties where B-site is modified with Ti/Fe/Co ions [9–12]. In other words, by doping rare-earth ions for A-site and magnetic ions in B- sites were found to have room temperature (RT) multiferroic applications and therefore these materials are referred to as future bismuth layered structure ferroelectromagnetic (BLSFEM) materials [8–16].

In view of the aforementioned importance of BLSFEM, many researchers were concentrating, globally, to improve electrical and magnetic properties by adopting the following strategy:

- i. Doping A-site with rare earth (RE) ions.
- ii. Magnetic ion (Co/Fe) doping at B (Ti)-site.
- iii. Adopting the intergrowth method between two different layer compounds.

The intergrowth of the BLSFEM compound consists of one unit cell of one-half the unit cell of m-layered and the other half unit cell of (m+1) layered compounds along the c-axis [6,17]. Earlier we reported the electrical properties of intergrowth of Sm-modified Bi₄Ti₃O₁₂ and SrBi₄Ti₄O₁₅ [17]. The XRD pattern of intergrowth is well indexed with the SrBi₃Ti₂O₂₂ (eight layers) compound. The same results were reported on similar compounds [18,19]. Kikuchi et al. [20] reported that the regular structure for higher-layer compounds m≥5, is built up of regular intergrowth of two layers of compounds of m and (m+1) in the common direction of the c-axis. They coined these compounds as a mixed-layered compounds and the structure can be written as:

$$(Bi_2O_2)^{2+}(A_{n-1}B_nO_{3n+1})^{2-}-(Bi_2O_2)^{2+}(A_{m-1}B_mO_{3m+1})^{2-} \qquad or \ Bi_4A_{m+n-2}B_{m+n}O_{3(m+n)+6}.$$

Here, the terms m and n represent the perovskite layers. It should remember here that the sum of 'm' and 'n' should be an even layer compound. Based on this, one can presume that SrBi₈Ti₇O₂₇ is built up with a mixed layer or intergrowth of m=3 and m=4 [20]. However, the plausible reason for the intergrowth structure of high-layer compounds is not known completely. On account of the complexity of the structure, a large number of layer compounds (m≥5) are being prepared by adopting the intergrowth route [21-23]. It was also reported that the ferroelectric properties of intergrowth compounds have shown higher ferroelectric properties compared to that of reactant layer compounds namely 3- and 4- layers compounds [7]. A recent report by Zhang et al [8] revealed that multiferroic intergrowth formed out of Bi3NdTi2Fe1-xCoxO12-8-Bi4NdTi3Fe1-xCoxO15(x=0.1-0.7) have shown higher magnetic and magnetoelectric (ME) properties for x=0.3. From transmission electron microscopy, it was reported modulation of 3 and 4-layered stacking sequences can be altered based on the cobalt content (x); alternative 4 and 3 for x=0.5, a dominant 3-layer for x=0.7 [8]. They found that the Co-ion substitution in the phase of Fe (for B-site) has shown higher ferromagnetic and magnetoelectric properties [8]. In view of this, many researchers [21-31] are preparing Co/Fe-modified (at B-site) compounds, and therefore intergrowth route is considered to be an effective way to improve ferroic properties, especially in Aurivillius materials.

In view of the significant ME coupling of the intergrowths based on the cobalt content, we chose the composition of Bi₃NdTi₂Fe_{0.7}Co_{0.3}O₁₂₋₈ - Bi₄NdTi₃Fe_{0.7}Co_{0.3}O₁₅ as a parent compound. Since rare-earth replacement at the Bismuth site in Aurivillius is known to reduce oxygen vacancies, [5,32,33] different rare earth ions, namely Dy, La, and Sm were doped at the A – site for the improved magnetoelectric coefficient. Detailed phase quantification, magnetization, and ME coupling are presented for different compositions.

2. Materials and Methods

Aurivillius phase of intergrowth compounds $Bi_3RTi_2Fe_{0.7}Co_{0.3}O_{12-\delta}$ - $Bi_4RTi_3Fe_{0.7}Co_{0.3}O_{15}$ (rare earth; R = Dy, Sm, and La) were prepared by conventional solid-

state reaction method. Initially, high-purity reactant oxides of Bi₂O₃, Dy₂O₃, Sm₂O₃, La₂O₃, TiO₂, Fe₂O₃, and Co₃O₄dried at 100 °C for 6h, were used to prepare 3-layered (Bi₃RTi₂Fe_{0.7}Co_{0.3}O_{12-δ}) and 4-layered (Bi₄RTi₃Fe_{0.7}Co_{0.3}O₁₅) compounds. The mixed powders were calcined at 850°C for 4 hours and subsequently grounded for 12 hours in the ball mill. The resultant compounds were analyzed for phase conformation by XRD measurements. Prior to the intergrowth formation, the prepared 3- and 4- layered compounds were taken in stoichiometric ratio and milled for 12 hours in the planetary ball mill. The present intergrowth compounds Bi₃RTi₂Fe_{0.7}Co_{0.3}O_{12-δ} - Bi₄RTi₃Fe_{0.7}Co_{0.3}O₁₅ (rare earth, R=Dy, Sm, and La) are named BDTFC, BSTFC, and BLTFC respectively. All the compounds were characterized by Powder X-ray diffraction using Cu Kα₁ radiation. The sintered powders were made into pellets of diameter, and thickness around 10mm, and 1mm respectively, and employed final- sintering at 900°C for 4 hours.

Powder X-ray diffraction was employed for the conformation of phase using a PANalytic X'Pert³ diffractometer. The XRD data was refined using FullProf Suite software. The surface morphology and EDAX (Energy Dispersive X-ray Spectroscopy) of the samples were studied using the ZEISS-EVO185SEM instrument. The grain sizes of the prepared samples were analyzed using ImageJ software and employed a histogram with Gaussian distribution. The structural evaluation was further studied by means of Raman spectroscopy using a Jobin-Yvon spectrometer (Horiba) using a 532 nm excitation laser. The magnetic measurements were carried out on all samples using under varying external magnetic fields using a vibrating sample magnetometer (VSM, cryogenic, UK.). ME studies were measured using, Micro-Measurement Group Strain Indicator, Model 3800, and series WK strain gauge. The ferroelectric polarization–electric field (P-E) was studied under different driving voltages using a P-E loop tracer (Radiant technologies). All samples were electrically poled under 10 kV/cm and magnetically at 5 kOe for 30 minutes each, prior to ferroelectric and magnetoelectric studies.

3. Results

3.1. Powder X-ray Diffraction and Morphological Studies

To confirm the single-phase purity, XRD was carried out in the range of 20° - 80° with a scan speed of 0.1°/min. The XRD patterns of both 3- layered compounds (Bi₃RTi₂Fe₀¬Co₀₃O₁₂-δ, R= Dy, La, and Sm) and 4- layered compounds (Bi₄RTi₃Fe₀¬Co₀₃O₁₅, R= Dy, La, and Sm) were used in Rietveld refinement. Figure 1(a-c) shows the XRD refinement of BDTFC, BLTFC, and BSTFC compounds. The lattice parameters were calculated by giving both space groups of 3-layered and 4-layered compounds. The compounds were found to be orthorhombic phase groups of A2₁am and b2cb with mixed phases of both 3- and 4-layered compounds. A detailed Rietveld analysis is made on these samples and the parameters were given in Fig 1. The Bragg peaks were fitted very well with the expected error with varying the size of rare earth ions [27,28]. The variation of lattice parameters and volume fraction of 3- and 4- layered phases with rare earth size is shown in Figure 2(a-c). Parameters for 3-layer and 4-layer with respect to the rare earth ion incorporation for Bi-site are shown in Figure 2. The volume fraction for the 4-layer phase is found to decrease, whereas, for the 3-layer phase it increases with an increase in ionic size.

From the plot, the overall phase contribution is found to be 4-layered (see Fig 2b), and the results were consistent with the reported HAADF images [8].

A good matching between theoretical and experimental XRD peaks was demonstrated by showing reliability factors within the reliable range (>10) [8]. Based on this observation one can conclude that the presence of pyrochlore formation is mainly due to the mixed valence combination of Fe and Co ions. It should remember here that the Ti, Fe, and Co cations were occupied at the B-site (center of each layer- perovskite) with fixed occupancy.

It is a known fact that Ti⁴⁺, Co²⁺, and Fe³⁺ cations are distributed randomly at the center position of octahedral for both 3-and 4-layered compounds. A partial substitution of

rare earth (R^{3+}) ion with Bi^{3+} certainly affects the structural changes. To confirm the quantification of the second phase, detailed EDAX images were shown in Figure 3.

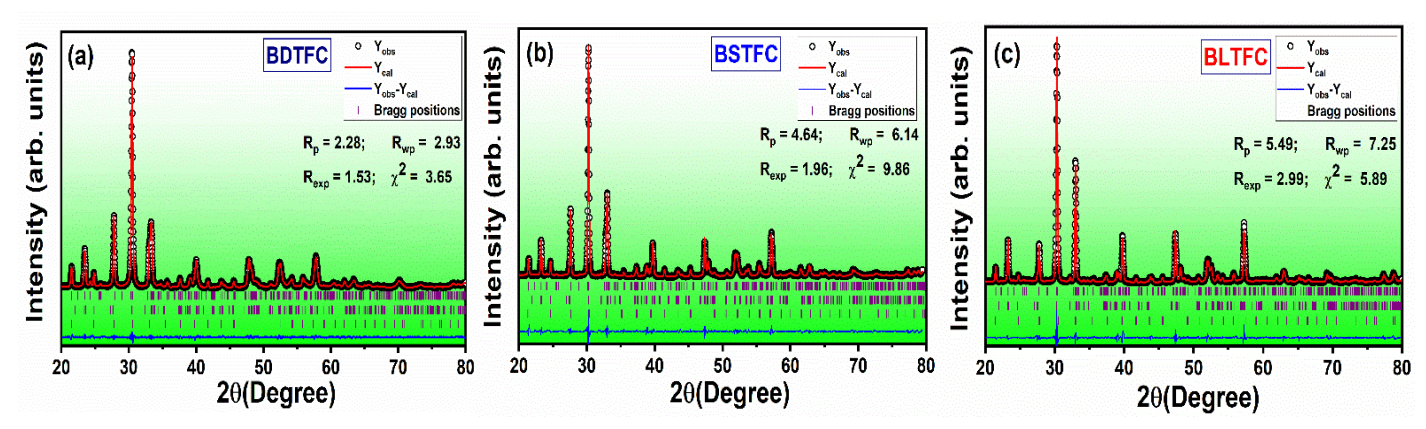


Figure 1. a-c) XRD patterns of the BDTFC, BSTFC, and BLTFC ceramics.

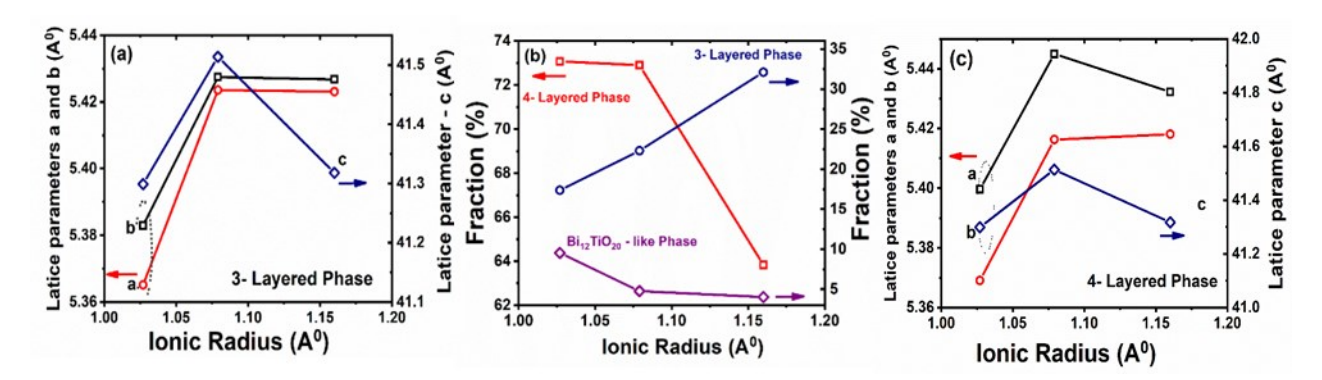


Figure 2. a-c) lattice parameters of (a) 3-layered phase and (b) 4- layered phase; (c) the volume fraction 3-, 4- layered, and impurity phase Bi₁₂TiO₂₀ phases with respect to rare earth ion size.

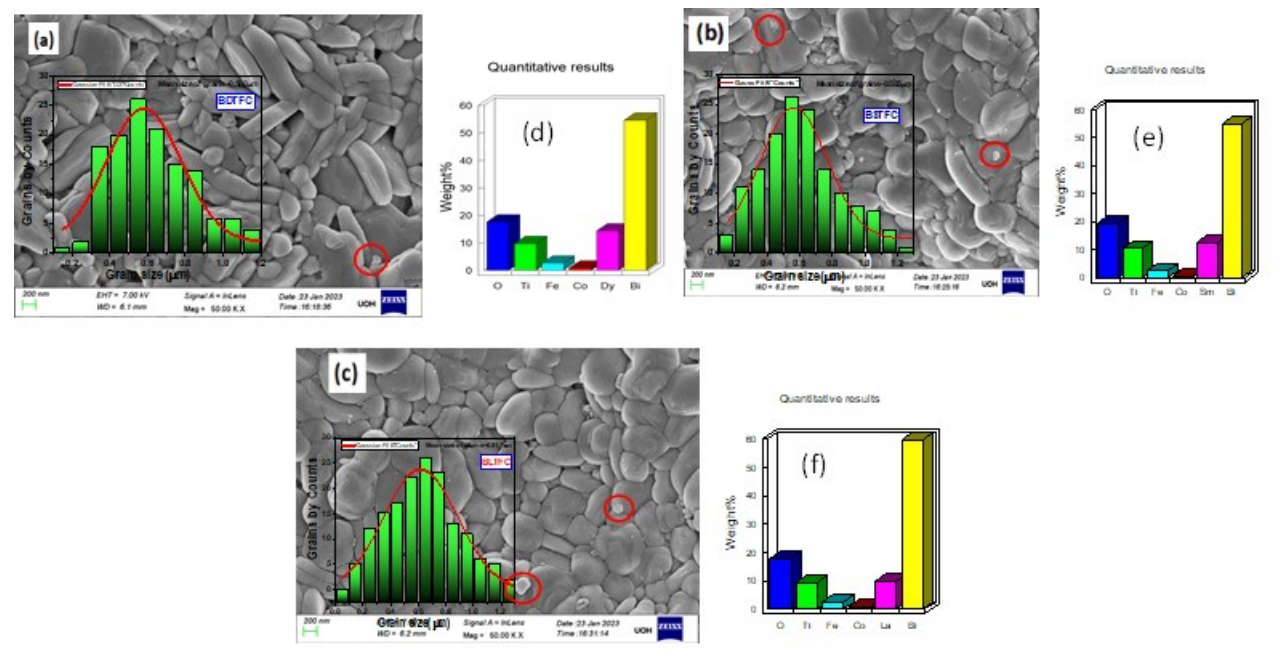


Figure 3. a-c) SEM images and grain size distribution of BDTFC, BSTFC, and BLTFC. **(d-f)** EDAX of BDTFC, BSTFC, and BLTFC samples.

From the images, it is evident that spots were observed. The orientation of randomly oriented plate-like morphology is also evident in the SEM images. In addition, a small spot (shown as encircle) of grain-like growth is also seen in the images. This kind of detected morphology is attributed to the accumulation of polyhedral phases of impurity phase or Co-Fe segregation at the grain boundary region [8]. The appearance of the secondary- phase affects the grain growth and leads to plate-like morphology with increasing the RE incorporation. The ratio of Fe/Co content found in the elemental analysis, shown in Figure 3(d-f), is found to be less than unity. This conforms to the collection of polyhedral grain over the SEM morphology, as shown as a circled region. Based on this observation one can conclude that the presence of pyrochlore formation is mainly due to the mixed value combination of Fe/Co and its ratio.

3.2. Raman Spectroscopic Studies

To understand the local structural properties, Raman spectroscopic analysis is made in the present investigation. Figure 4 (a-c) shows the Raman spectra of BDTFC, BSTFC, and BLTFC samples respectively. The spectral phonon peaks above 200cm⁻¹ marked as v₄ are assigned to the internal mode of TiO₆ octahedra. A small shift in the fitted peak position indicates that RE⁺³ ion participation in place of Bi⁺³ ion. The broad valley-like behavior observed between 300cm⁻¹ and 400cm⁻¹ indicates the diffusion of Co/Fe content. Appearing two peaks, near 550cm⁻¹, is mainly due to the substitution of Fe/Co at the Ti-site. It is difficult to explain each phonon mode and its overlapping with weak intensity. The detailed phonon modes indicated in Figure 4 are almost well-matched with the literature [29–31].

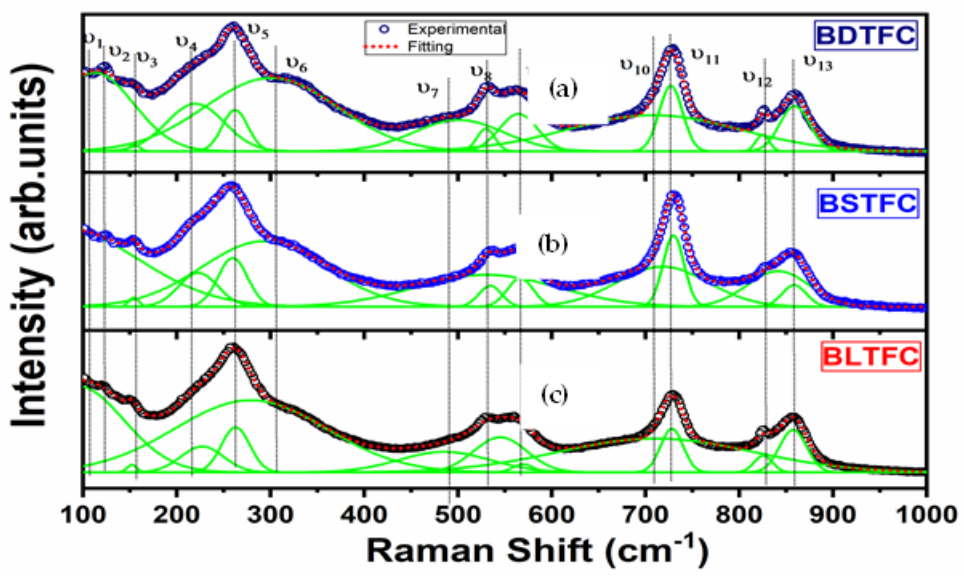


Figure 4. (a-c). Raman spectra of BDTFC, BSTFC, and BLTFC samples.

The modes observed at 260cm^{-1} (v₃) are attributed to the internal angles torsional bending of (Ti/Fe/Co)O₆ bonding. The modes observed at 360cm^{-1} (v₆) are due to the stretching vibration of oxygen along the c-axis (O-Ti/Fe/Co-O) stretching mode. The mode v₇ (470 cm⁻¹) is due to changes that occurred in the bond distance Bi atom within the Bi₂O₂ layer and its apical O-atom of the perovskite block. Two nearby modes v₈ and v₉ observed at 540cm^{-1} and 560cm^{-1} are due to the physically opposing oxygen atom from TiO₆ octahedral [29,32–34]. The stretching modes of Bi/RE-O stand in A-site shows modes at v₁₀ and v₁₁. The last modes v₁₂ and v₁₃ are related to once again bonding of stretching of octahedral. The overall Raman peaks and a slight notable difference observed near v₁-v₃ (low region) are attributed to A-site cation and Bi/RE⁺³ ion variation in the (Bi₂O₂)²⁺ layers. The results also suggest the rare earth ion readily substitutes within the Bi⁺³ ion [26]. The peaks near

 v_8 and v_9 are attributed to the decrease in the fitted octahedral distortion in (Ti/Fe/Co) O₆. The broad mode originating at 560 cm⁻¹ explains the substitution of RE ions at the A-site. An increase in the broadness of peak or more tendency of convolution is observed with decreasing the rare earth ion substitution for the Bi (A-) site. An increase in the intensity of the v_9 peak indicates more structural distortion and improves the competitive electric-magnetic interactions.

3.3. Ferroelectric Studies

The Hysteresis loop (Polarization (P)-Electric field (E)) of BDTFC, BSTFC, and BLTFC samples are shown in Fig 5(a-c). The measurements were performed at different voltages as depicted in the plot. The shapes of the hysteresis loops were found to be sharp at the edges. It is a known fact that the coercive and saturation fields of Aurivillius materials are very high. The piezoelectric properties (d33) of BLSFEM are generally low (~ 50 pC/N). To improve d33 and ferroelectric properties different rare earth ions were substituted for the Bi³⁺ site. If the Bi³⁺/RE³⁺ ratio increases then the deformation of the octahedron of layerperovskite alters the dipole moment as well as depolarization properties. Finally, all the ordering of these materials tunes to multiferroic applications. The unsaturated and nonsymmetric nature of loops is associated with the leaky nature, on account of the high concentration of oxygen vacancies [7,17]. It is also observed that the coercive field and polarization increase with the applied voltages, as shown in Figure 5(a-c). In addition, when Ti ions get replaced with Co /Fe ions, they form defect complexes such as Fe3+-Vo-Fe3+ and Co²⁺-Vo-Co²⁺. Thus, the oxygen vacancies get trapped by Fe³⁺ and Co²⁺ ions and hence they require a higher electric field to exhibit saturated hysteresis loops [35]. Unfortunately, it was not possible to apply a high electric field on account of the limitation of the instrument. Despite these limitations, all samples have shown ferroelectric loops without a signature of a loss nature.

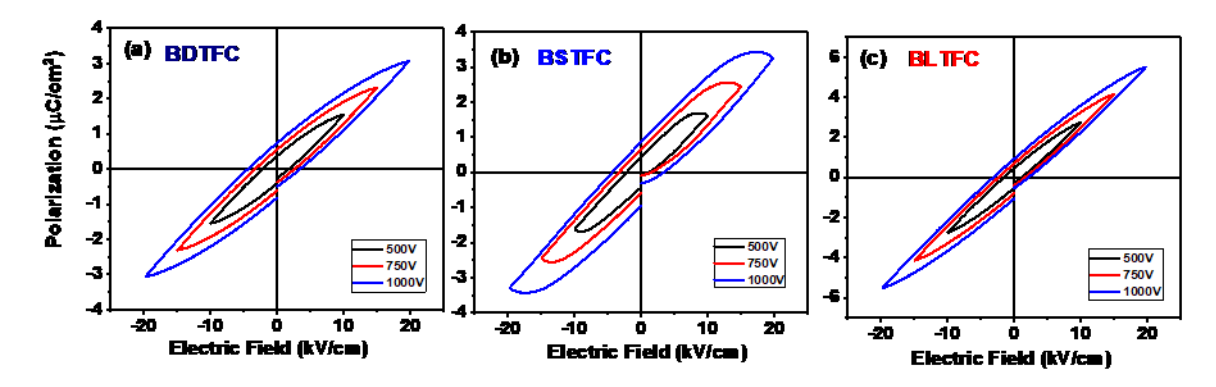


Figure 5. a-c). Ferroelectric hysteresis loops (P vs E curves) of BDTFC, BSTFC, and BLTFC samples.

3.4. Magnetic Studies

It is a known fact that the electric and magnetic interaction originates from the exchange interaction between neighboring Fe³⁺- O-Co⁺² ions. Room temperature magnetic hysteresis curves are shown in Figure 6(a-c). It is reported in the literature that these materials belong to a canted AFM (anti-ferromagnetism) nature. On account of the canted nature, these materials have small net magnetization with an at-most saturated region at higher magnetic fields [34–36]. The antiferromagnetic nature is attributed on account of tilt-canted spins, and can be understood by the following equation:

$$\sigma = \sigma_P + \chi H \qquad ---- \tag{1}$$

Here σ is total magnetic moment, σ_P is weak ferromagnetic moment and χH represents antiferromagnetic component. The canted AFM nature is generally verified with the help of the following facts:

- i. At low temperatures, the M-H loop resembles with ferromagnetic (FM) hysteresis loop.
- ii. At higher magnetic fields, the magnetization shows linear behavior with the magnetic field.
- iii. At higher magnetic fields, magnetization vs. magnetic field data shows a linear increase due to nearby magnetic ion interaction, namely iron (Fe) and cobalt (Co).
- iv. The strength of magnetic nature can be understood by the law approach to saturation. This gives additional information about anisotropic properties.

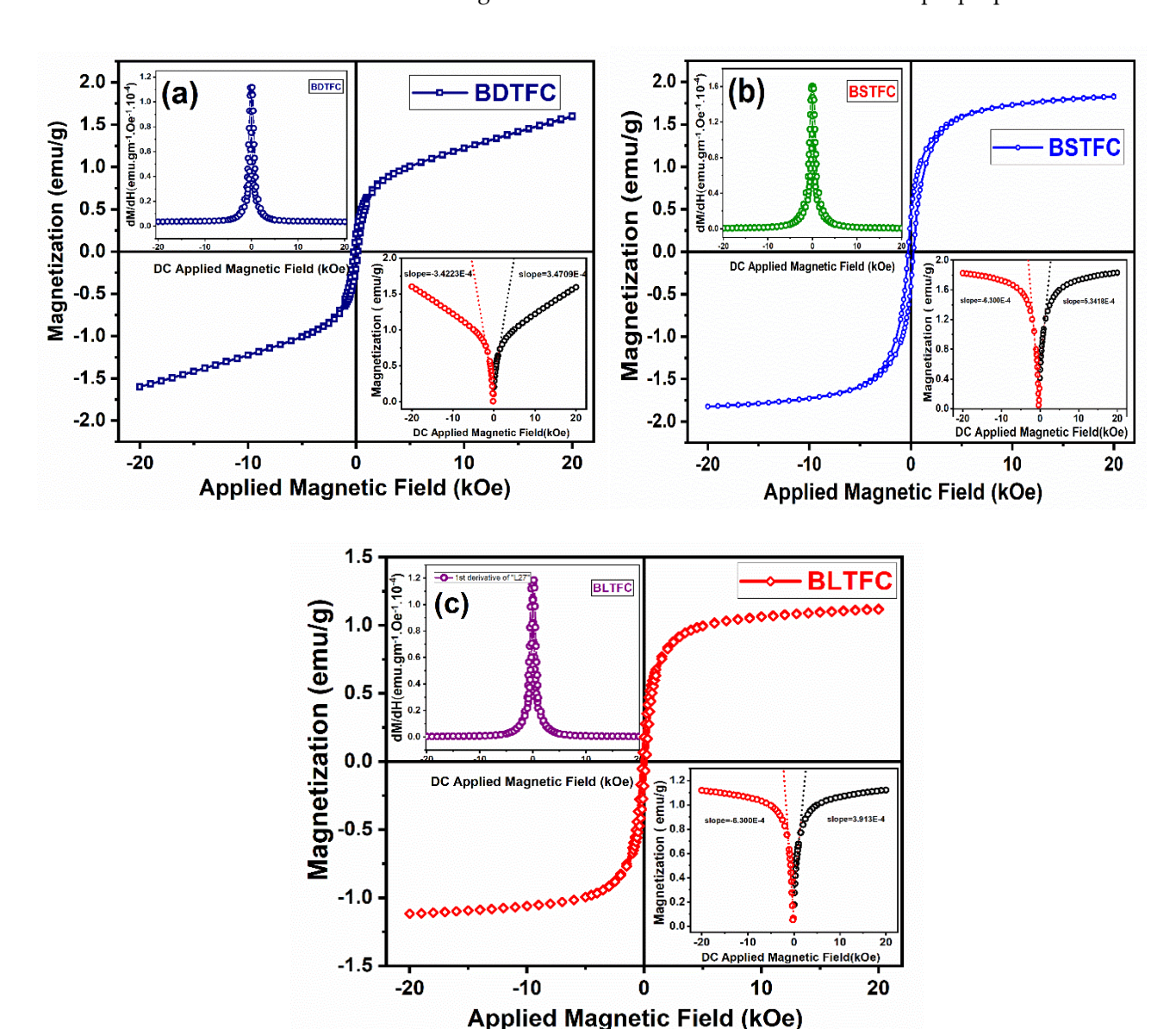


Figure 6. a-c). Magnetic hysteresis loops (M vs H curves) of BDTFC, BSTFC, and BLTFC samples.

Table 6. The magnetization values were found to be high when compared to the parent compound [8]. The high magnetization values were attributed to the structural distortion and domain orientations. The canted AFM or weak ferromagnetic nature is attributed to the canting spin of Fe-Co-Fe interaction or Dzyaloshins-Mariya interaction. Based on the magnetic nature of RE ions, a higher value of magnetization is observed for BSTFC. The results were consistent with the literature [37].

In the present investigation showing saturated behavior at higher fields clearly indicates a spin canting and the movement of cations between given bonding (Fe/Co) plays a

role to give net saturation. The saturation magnetization is generally employed by fitting the isotherm data shown in Figure 7 (a-c). At lower fields, (H/M) saturation magnetization curves tend to have a finite positive value. The positive intercept indicates the weak ferromagnetic nature [37]. To separate out the FM and AFM contribution in the sample, the following relation is used,

$$M(H) = \left[2 \frac{M_{FM}^S}{\pi} \tan^{-1} \left\{ \left(\frac{M \pm M_{CI}}{M_{CI}} \right) \tan \left(\frac{\pi M_{FM}^R}{2 M_{FM}^S} \right) \right\} \right] + \chi H \tag{2}$$
 The term M_{FM}^S represents FM saturation magnetization, M_{FM}^R represents remanent

magnetization. The last term χ represents the AFM contribution part.

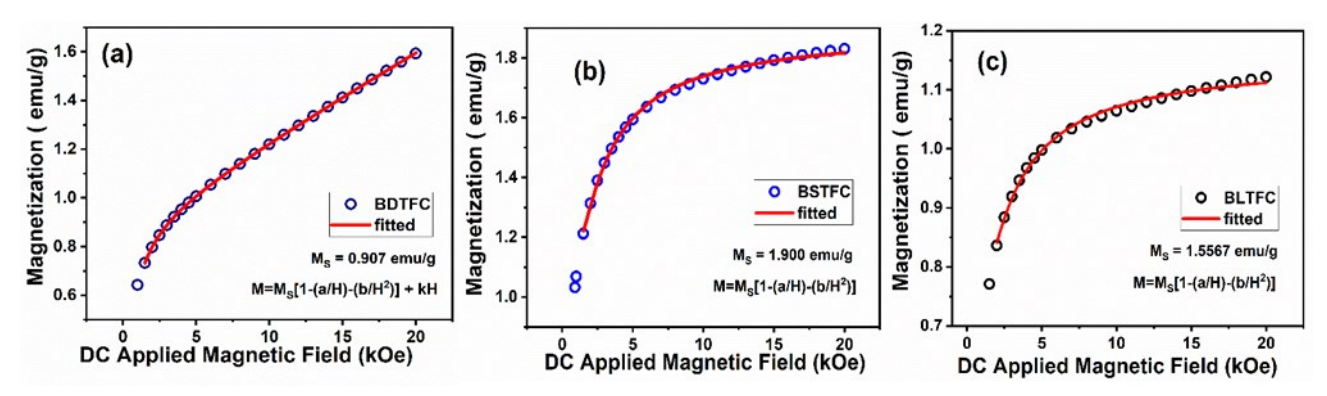


Figure 7. a-c). Law of approach to saturation fittings M vs H curves of BDTFC, BSTFC, and BLTFC samples.

From equation (2) the first term represents FM nature and the second term indicates AFM part of strong. Here the strong spin interaction FM nature, and it becomes weak. To extract more information about FM nature and its anisotropy, the law of approach to saturation technique is used [38–42]:

$$M = M_s \left(1 - \frac{A}{M} - \frac{B}{M^2} + kH \right) \tag{3}$$

Anisotropy field (M_K) can be estimated from the following formula: $M_k = \frac{2k_i}{\mu_0 M_S}$

$$M_k = \frac{2k_i}{\mu_0 M_S} \tag{4}$$

The Inset of Figure 6(left) shows the variation of (dM/dH) with the applied field of all samples. Inset Figure 6(right) shows variation magnetization (Ms) with the applied magnetic field. All dM/dH curves show a single sharp peak at the origin. From this, one can speculate that all prepared samples have a single magnetic grain type and are of soft magnetic nature. It should remember that the Co+3 doping with Fe concentration is the same for all the samples (BDTFC, BSTFC, BLTFC), and the two slopes found at the origin explain the magnetic linkage between Fe/Co magnetic grains of layered perovskites. The presence of nanoregions which were raked as Fe, and Co rich observed as dots in SEM pictures. The calculated ratio of intergrowth grains and magnetic nanoregions of all the samples was found to be less than 0.1.

Low-temperature magnetization by zero-field cooled (ZFC) and field cooled (FC) sequences were measured under a small external magnetic field (1kOe) in the range of 2 to 300K, which are shown in Figure 8 (a-c). The increase in M (magnetization) with decreasing temperature clearly indicates the stability and strong coupling interaction between magnetic dipoles at those temperatures (shown as inset Figure 8(a-c)). The divergence of ZFC and FC curves is generally attributed to the signature AFM (Antiferromagnetic) nature. In the present case, dispersion is shown in Figure 8 clearly indicating canted AFM nature.

The radius of $Co^{2+}(0.745A^0)$ is larger when compared to $Fe^{2+}(0.605A^0)$. The Co^{2+} substitution for Ti- ion creates oxygen vacancies [8,27]. From this one can speculate Ti³⁺-O-Ti⁴⁺ decreases the bond angle and finally weakens the magnetic exchange interaction. This leads to a decrease in the magnetic order and its interaction. Moreover, a noteworthy aspect observed in the plot of the ZFC and FC condition plot clearly confirms that magnetic weak or superparamagnetic or canted AFM nature. Similar results were also observed in the Bi₆FeCoTi₅O₁₈ compound [26].

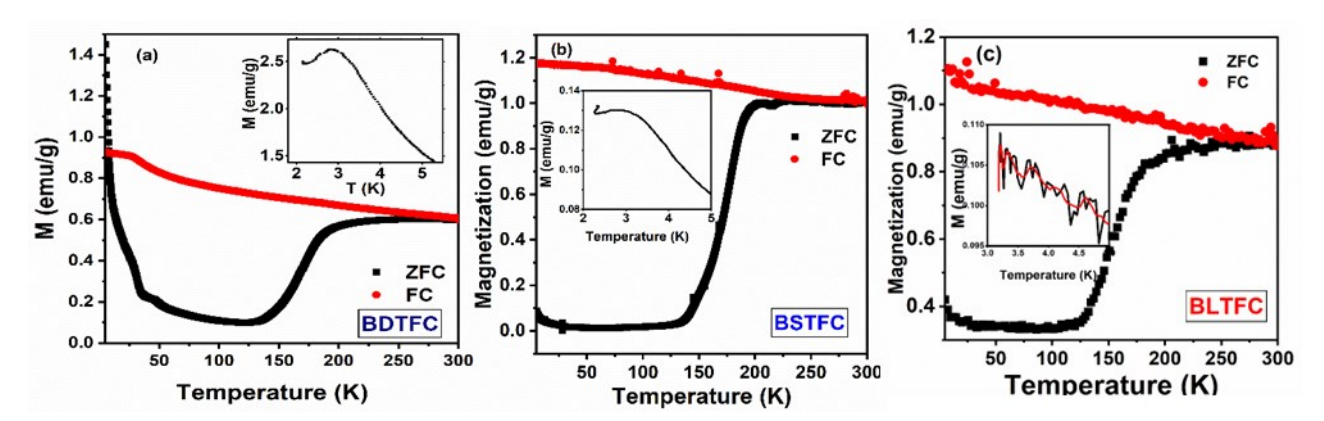


Figure 8. a-c).Temperature dependence of magnetization curves for BSTFC sample measured in the ZFC and FC.

3.5. Magnetoelectric Studies

Figure 9 shows the magnetic field dependence of the magnetoelectric (ME) coefficient at room temperature. An ac frequency 550Hz was applied prior to the extraction of ME data. The value of the ME coefficient has been found 27mV/cm-Oe, 21mV/cm-Oe, and 14mV/cm-Oe for BSTFC, BDTFC, and BLTFC respectively. Moreover, the ME coefficient was found to be almost constant throughout the measurement in the positive magnetic field [42]. Both magnetic and magnetoelectric properties of the studied compositions were shown enhanced results compared to the parent compound.

BSTFC compound has shown a higher ME coefficient compared to the other samples. The value is found to be higher than the parent compound (1 mV/Cm-Oe) [8]. From this one can speculate that the intrinsic nature of magnetoelectric interaction could possibly be due to magnetic and electric interaction, driven by inverse DM interaction or spin–orbit and spin exchange interaction. The cause of ME coupling, however, is yet to be explored.

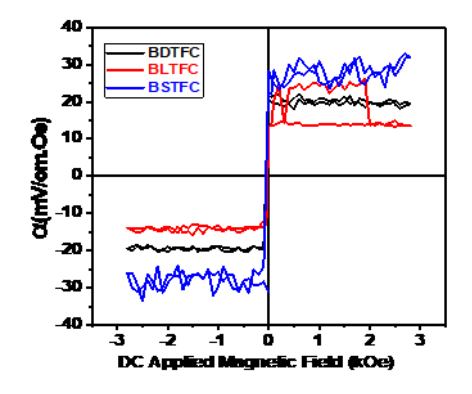


Figure 9. Magnetic field dependence of the magnetoelectric (ME) coefficient at room temperature for BDTFC, BSTFC, and BLTFC samples.

As mentioned earlier, we found nanoregions in the SEM images of the samples. Such nanoregions are also reported in earlier reports corresponding to the Co_xFe_y composition resulting from the synthesis. Zhang et al [8] also observed the occurrence of a similar phase from their SEM observations which are consistent with the current study. It can be speculated here from the ME coupling effects can be due to the formation of CoxFey phases.

Given the similar conditions of materials synthesis for all the three rare-earth doped samples in this study, one can expect same the amount of Co_xFe_y phase in all these

samples. In this scenario, the improved ME response observed for Sm-based intergrowth arises out of structural distortion. The tetragonal strain, orthorhombocity, and orthorhombic distortions play a major role in the polarization switching of Aurivillius oxides in view of octahedral distortions [33]. The replacement of Sm, La, Dy at the A-site has resulted in the orthorhombic distortion(b/a), tetragonal strain (c/a), and ortho-rhombocity (2(ab)/(a+b)) of (0.9947,0.9974, 0.9943 for 4-layered phase& 0.9993, 0.9993,0.997 for 3 layered phase), (7.6242, 7.606, 7.6484 for 4-layered phase & 5.989, 5.963, 6.001 for 3-layered phase), and (0.0053, 0.0026, 0.0056 for 4 layered phase & 0.0007, 0.0007 0.0033 for 3-layered phase) respectively. Stable orthorhombocity and lower orthorhombic distortions for Sm, Dybased intergrowths seem to be favorable for polarization switching under magnetic fields. It is also evident that the ME output is strongly dependent on the volume fraction and the existence of both 3-layered and 4-layered phase structures in the present intergrowth compounds. From this, one can conclude that the intergrowth rare earth-doped compounds have shown strong ME coupling in the Aurivillius multiferroic phases. Higher magnetization accompanied by a ferroelectric polarization induced by the structural distortions for Sm, Dy. This intern leads to higher ME coupling.

4. Conclusions

After adding the stoichiometric amounts of the three-layered and four-layered compounds, we have prepared intergrowth compounds named BDTFC, BLTFC, and BSTFC respectively. The intergrowth compounds have been found to be single phase and the structure of the compound is mixed phases of 3- and 4-layered compounds. In our earlier results, and in the literature, it is also reported that the intergrowth of 3- and 4-layered compounds form an 8-layer compound. The reason for the intergrowth structure is still debatable and therefore high-layer compounds will certainly open up a new direction in the multiferroic fields.

Based on the magnetic and magnetoelectric results, one can conclude that the origin of the weak ferromagnetic nature is attributed to the mixed valence states of +2 and +3 of Fe and Co ions. The possible neighboring exchange interaction between iron and cobalt is Fe^{+3} -O-Co⁺², Co^{+3} -O-Co⁺², and Co^{+3} -O-Fe⁺². In addition to that, Fe^{+3} -O-Fe⁺² indicates AFM superexchange interaction. The canted spin nature, especially in Co and Fe mixed phases is generally observed in these materials, called DM interaction. Doping of RE⁺³ ions causes $(Fe/Co)O_6$ octahedral tilt and hence DM interaction play a dominant part. Substituting trivalent Co ion in place of Fe ion generally improves strong magnetic interaction. Intergrowth materials were found to be single domain and soft magnetic type. These multiferroic materials are important candidates for advanced multi-functional sensors.

Author Contributions: V.Veenachary, N.V. Prasad, and E.V. Ramana: Conceptualization, Methodology, Data curation, Writing – original draft and reviewed work, Investigation. N.V. Prasad, G Prasad, and A Srinivas supervised this work. S.N. Babu and Venkata Sreenivas Puli helped in the Raman Spectroscopy investigation. Venkata Sreenivas Puli, Gopalan Srinivasan, and Sujoy Saha helped with ME coupling measurements.

Funding:This work was partially supported by OU-DSTPURSUE-II/80//2021 and CSIR-HRDG, No: 09/132(0875)/2018-EMR-I, New Delhi for providingFellowship. The research at Oakland University was supported by grants from the National Science Foundation (DMR-1808892, ECCS-1923732) and the Air Force Office of Scientific Research (AFOSR) Award No. FA9550-20-1-0114. The author, VSP acknowledges National Research Council (NRC) senior research associate fellowship program. This work was supported in part by the Air Force Office of Scientific Research and by the Air Force Research Laboratory.

Data Availability Statement: Not applicable

Acknowledgments: One author (V Veenachary) is thankful to CSIR-HRDG, New Delhi for providing JRF/SRF (FileNo: 09/132(0875)/2018-EMR-I). One of the authors (N.V.Prasad) thanks and acknowledges DST for partial funding by the grants from OU-DST PURSUE-II/ 80/2021 program. EVR (032-88-ARH/2018) acknowledges the Portuguese foundation for science and

technology (FCT) for financial assistance through national funds (OE), in the scope of the framework contract foreseen in the numbers 4, 5, and 6 of article 23 of the Decree-Law 57/2016, of August 29, changed by Law 57/2017, of July 19.

Conflicts of Interest: The authors declare no conflict of interest.

References

- Subbarao, E.C. A Family of Ferroelectric Bismuth Compounds. J. Phys. Chem. Solids 1962, 23, 665–676 https://doi.org/10.1016/0022-3697(62)90526-7.
- ^{2.} Sun, S.; Yin, X. Progress and Perspectives on Aurivillius-type Layered Ferroelectric Oxides in Binary Bi4Ti₃O₁₂-BiFeO₃ System for Multifunctional Applications. *Crystals* **2021**, *11*, 23.
- Sun, J.; Han, Y.; Gao, G.; Yang, J.; Zhang, Y.; Dai, Y.; Song, D. Breakdown Field Enhancement and Energy Storage Performance in Four-Layered Aurivillius Films. *Ceram. Int.* **2022**, *48*, 15780–15784. https://doi.org/10.1016/j.ceramint.2022.02.115.
- Gao, X.; Gu, H.; Li, Y.X.; Yi, Z.G.; Čeh, M.; Žagar, K. Structural Evolution of the Intergrowth Bismuth-Layered Bi₇Ti₄NbO₂₁. J. Mater. Sci. 2011, 46, 5423–5431. https://doi.org/10.1007/s10853-011-5483-y.
- 5. Ramana, E.V.; Prasad, N.V.; Tobaldi, D.M.; Zavašnik, J.; Singh, M.K.; Hortigüela, M.J.; Seabra, M.P.; Prasad, G.; Valente, M.A. Effect of Samarium and Vanadium Co-Doping on Structure, Ferroelectric and Photocatalytic Properties of Bismuth Titanate. RSC Adv. 2017, 7, 9680–9692. https://doi.org/10.1039/c7ra00021a.
- Noguchi, Y.; Miyayama, M.; Kudo, T. Ferroelectric Properties of Intergrowth Bi₄Ti₃O₁₂-SrBi₄Ti₄O₁₅ Ceramics. *Appl. Phys. Lett.* **2000**, 77, 3639–3641. https://doi.org/10.1063/1.1328366.
- Parida, G.; Bera, J. Electrical Properties of Niobium Doped Bi₄Ti₃O₁₂-SrBi₄Ti₄O₁₅ Intergrowth Ferroelectrics. *Ceram. Int.* **2014**, *40*, 3139–3144. https://doi.org/10.1016/J.CERAMINT.2013.09.131.
- 8. Zhang, D.L.; Huang, W.C.; Chen, Z.W.; Zhao, W.B.; Feng, L.; Li, M.; Yin, Y.W.; Dong, S.N.; Li, X.G. Structure Evolution and Multiferroic Properties in Cobalt Doped Bi₄NdTi₃Fe_{1-x}CoO₁₅-Bi₃NdTi₂Fe_{1-x}Co_xO_{12-δ} Intergrowth Aurivillius Compounds. Sci. Rep. 2017, 7, 43540. https://doi.org/10.1038/srep43540.
- Paul, J.; Bhardwaj, S.; Sharma, K.K.; Kotnala, R.K.; Kumar, R. Room-Temperature Multiferroic Properties and Magnetoelectric Coupling in Bi4-xSmxTi3-xCoxO12-b Ceramics. J. Mater. Sci. 2014, 49, 6056–6066. https://doi.org/10.1007/s10853-014-8328-7.
- Rehman, F.; Li, J.B.; Dou, Y.K.; Zhang, J.S.; Zhao, Y.J.; Rizwan, M.; Khalid, S.; Jin, H.B. Dielectric Relaxations and Electrical Properties of Aurivillius Bi3.5La0.5Ti2Fe0.5Nb0.5O12 Ceramics. J. Alloys Compd. 2016, 654, 315–320. https://doi.org/10.1016/j.jall-com.2015.07.181.
- Bai, W.; Yin, W.; Yang, J.; Tang, K.; Zhang, Y.; Lin, T.; Meng, X.; Duan, C.G.; Tang, X.; Chu, J. Cryogenic Temperature Relaxor-like Dielectric Responses and Magnetodielectric Coupling in Aurivillius Bi₅Ti₃FeO₁₅ Multiferroic Thin Films. *J. Appl. Phys.* **2014**, 116, 084103. https://doi.org/10.1063/1.4893710.
- Nazemian, M.; Khoshnoud, D.S. The Enhanced of Magnetic and Electrical Properties of Bi₅FeTi₃O₁₅ Compound with Replacing Co for Ti Sites. *J. Magn. Magn. Mater.* **2023**, *565*, 170243. https://doi.org/10.1016/j.jmmm.2022.170243.
- Paul, J.; Bhardwaj, S.; Sharma, K.K.; Kotnala, R.K.; Kumar, R. Room Temperature Multiferroic Properties and Magnetoelectric Coupling in Sm and Ni Substituted Bi4xSmxTi3-xNi xO12±6 (x = 0, 0.02, 0.05, 0.07) Ceramics. *J. Appl. Phys.* **2014**, *115*, 204909. https://doi.org/10.1063/1.4880159.
- Yang, F.J.; Su, P.; Wei, C.; Chen, X.Q.; Yang, C.P.; Cao, W.Q. Large Magnetic Response in (Bi₄Nd)Ti₃(Fe_{0.5}Co_{0.5})O₁₅ Ceramic at Room-Temperature. J. Appl. Phys. 2011, 110, 126102. https://doi.org/10.1063/1.3671418.
- ^{15.} Yin, Y.; Liu, F.; Mao, X.; Wang, W. Multiferroic Properties of Bi5.75R0.25Fe1.4Ni0.6Ti3O18 (R = Eu, Sm, Nd, Bi and La) Ceramics. *J. Rare Earths* **2022**, *40*, 112–117. https://doi.org/10.1016/j.jre.2020.11.019.
- Alkathy, M.S.; Rahman, A.; Zabotto, F.L.; Milton, F.P.; Raju, K.C.J.; Eiras, J.A. Room-Temperature Multiferroic Behaviour in Co/Fe Co-Substituted Layer-Structured Aurivillius Phase Ceramics. Ceram. Int. 2022, 48, 30041–30051. https://doi.org/10.1016/j.ceramint.2022.06.273.
- Babu, B.S.; Babu, S.N.; Prasad, G.; Kumar, G.S.; Prasad, N.V. Structure and Dielectric Properties of Sm³⁺ Modified Bi₄Ti₃O₁₂-SrBi₄Ti₄O₁₅ Intergrowth Ferroelectrics. *Process. Appl. Ceram.* **2020**, *14*, 260–267. https://doi.org/10.2298/pac2003260s.
- ^{18.} Kharitonova, E.P.; Voronkova, V.I. Synthesis and Electrical Properties of Mixed-Layer Aurivillius Phases. *Inorg. Mater.* **2007**, 43, 1340–1344. https://doi.org/10.1134/S0020168507120175.
- Wang, L.; Gui, M.; Jin, H.B.; Hu, X.; Zhao, Y.; Adnan, N.M.; Li, J.B. Temperature Dependent Conductivity of Bi₄Ti₃O₁₂ Ceramics Induced by Sr Dopants. *J. Adv. Ceram.* 2018, 7, 256–265. https://doi.org/10.1007/s40145-018-0277-1.
- ^{20.} Kikuchi, T.; Watanabe, A.; Uchida, K. *A Family of Mixed-Layer Type Bismuth Compounds*; Pergamon Press, Inc. Oxford, UK, 1977; Volume 12.
- Hou, R.Z.; Chen, X.M.; Wu, S.Y. Substitution of Sm³+ and Nd³+ for Bi³+ in SrBi®Ti7O27 Mixed Aurivillius Phase. *Jpn. J. App. Phys. Part 1 Regul. Pap. Short Notes Rev. Pap.* **2003**, 42, 5169–5171. https://doi.org/10.1143/jjap.42.5169.
- Zurbuchen, M.A.; Podraza, N.J.; Schubert, J.; Jia, Y.; Schlom, D.G. Synthesis of the Superlattice Complex Oxide Sr₅Bi₄Ti₈O₂₇ and Its Band Gap Behavior. *Appl. Phys. Lett.* **2012**, *100*, 223109. https://doi.org/10.1063/1.4722942.
- Yan, J.; Hu, G.D. Enhanced Ferro-and Piezoelectric Properties of Bi₄Ti₃O₁₂-CaBi₄Ti₄O₁₅ Thin Film on Pt(111)/Ti/SiO₂/Si Substrate. *Mater. Res. Express* **2018**, *5*, 056306. https://doi.org/10.1088/2053-1591/aac4e7.

- ^{24.} Zhao, Y.; Li, Y.; Lu, Y.; Wang, Y. The Formation Mechanism of Intergrowth Bismuth Layer-Structured Ferroelectric Bi₄Ti₃O₁₂-CaBi₄Ti₄O₁₅. Ferroelectrics **2010**, 404, 45–49.
- Jiang, Y.; Jiang, X.; Chen, C.; Nie, X.; Huang, X.; Jiang, X.; Zhuang, J.; Zheng, L.; Chen, Z. Effect of Tantalum Substitution on the Structural and Electrical Properties of BaBisTizO2z Intergrowth Ceramics. Ceram. Int. 2020, 46, 8122–8129. https://doi.org/10.1016/j.ceramint.2019.12.039.
- Wang, G.; Yang, H.; Wang, J.; Sun, S.; Fu, Z.; Zhai, X.; Peng, R.; Knize, R.J.; Lu, Y. Engineering the Exchange Bias and Bias Temperature by Modulating the Spin Glassy State in Single Phase Bi₉Fe₅Ti₃O₂₇. *Nanoscale* **2017**, *9*, 8305–8313. https://doi.org/10.1039/c7nr02156a.
- ^{27.} Lomanova, N.A. Aurivillius Phases Bim+ 1Fem- 3Ti3O3m+ 3: Synthesis, Structure, and Properties (a Review). *Russ. J. Inorg. Chem.* **2022**, *67*, 741–753. https://doi.org/10.1134/S0036023622060146.
- ^{28.} Liu, F.; Jiang, X.; Chen, C.; Nie, X.; Huang, X.; Chen, Y.; Hu, H.; Su, C. Structural, Electrical and Photoluminescence Properties of Er³⁺-Doped SrBi₄Ti₄O₁₅—Bi₄Ti₃O₁₂ Inter-Growth Ceramics. *Front. Mater. Sci.* **2019**, *13*, 99–106. https://doi.org/10.1007/s11706-019-0454-3.
- Jiang, Y.; Jiang, X.; Chen, C.; Chen, Y.; Jiang, X.; Tu, N.; Xia, X.; Luo, Y.; Zhu, S. Structural and Electrical Properties of La³⁺-Doped Na_{0.5}Bi_{4.5}Ti₄O₁₅-Bi₄Ti₃O₁₂ Inter-Growth High Temperature Piezoceramics. *Ceram. Int.* 2017, 43, 6446–6452. https://doi.org/10.1016/j.ceramint.2017.02.059.
- Graves, P.R.; Hua, G.; Myhra, S.; Thompson, J.G. The Raman Modes of the Aurivillius Phases: Temperature and Polarization Dependence. *J. Solid State Chem.* **1995**, *114*, 112–122. https://doi.org/10.1006/jssc.1995.1017.
- Silva, P.H.T.; Silva, M.A.S.; da Silva, R.B.; Correa, M.A.; Bohn, F.; de Menezes, A.S.; Ferreira, W.C.; Ayala, A.P.; Sombra, A.S.B.; Fechine, P.B.A. Effects of the Bi3+ Substitution on the Structural, Vibrational, and Magnetic Properties of Bismuth Layer-Structured Ferroelectrics. *Appl. Phys. A* **2020**, *126*, 653. https://doi.org/10.1007/s00339-020-03858-y.
- Venkata Ramana, E.; Figueiras, F.; Graça, M.P.F.; Valente, M.A. Observation of Magnetoelectric Coupling and Local Piezore-sponse in Modified (Na_{0.5}Bi_{0.5})TiO₃–BaTiO₃–CoFe₂O₄ Lead-Free Composites. *Dalton Trans.* **2014**, 43, 9934–9943. https://doi.org/10.1039/C4DT00956H.
- Veenachary, V.; Puli, V.S.; Babu, S.N.; Prasad, G.; Prasad, N.V. Electrical and Magnetic Studies on Promising Aurivillius Intergrowth Compound. *J. Mater. Sci. Mater. Electron.* **2022**, *33*, 22614–22627. https://doi.org/10.1007/s10854-022-09039-2.
- Rodríguez Aranda, M.D.C.; Rodríguez-Vázquez, Á.G.; Salazar-Kuri, U.; Mendoza, M.E.; Navarro-Contreras, H.R. Raman Effect in Multiferroic Bi ⁵ Fe ^{1+x}Ti^{3-x}O ¹⁵ Solid Solutions: A Temperature Study. *J. Appl. Phys.* **2018**, 123, 084101. https://doi.org/10.1063/1.5019291.
- Basheer, M.A.; Gangadhar, V.; Prasad, G.; Kumar, G.S.; Prasad, N.V. Electrical and Raman Spectroscopic Studies on Aurivillius Layered-Pervoskite Ceramics. *Adv. Mater. Res.* **2019**, *1154*, 80–90. https://doi.org/10.4028/www.scientific.net/amr.1154.80.
- Wang, C.H.; Liu, Z.F.; Yu, L.; Tian, Z.M.; Yuan, S.L. Structural, Magnetic and Dielectric Properties of Bi_{5-x}La_xTi₃Co_{0.5}Fe_{0.5}O₁₅ Ceramics. *Mater. Sci. Eng. B Solid State Mater. Adv. Technol.* **2011**, *176*, 1243–1246. https://doi.org/10.1016/j.mseb.2011.06.016.
- Bobić, J.; Ilić, N.; Veerapandiyan, V.; Petrović, M.V.; Deluca, M.; Dzunuzović, A.; Vukmirović, J.; Ning, K.; Reichmann, K.; Tidrow, S. Tailoring the Ferroelectric and Magnetic Properties of Bi₅Ti₃FeO₁₅ Ceramics by Doping with Co and Y. *Solid State Sci.* **2022**, *123*, 106802. https://doi.org/10.1016/j.solidstatesciences.2021.106802.
- Wang, G.; Huang, Y.; Sun, S.; Wang, J.; Peng, R.; Lu, Y.; Tan, X. Layer Effects on the Magnetic Behaviors of Aurivillius Compounds Bin+1Fen-3Ti3O3n+1 (n = 6, 7, 8, 9). *J. Am. Ceram. Soc.* **2016**, 99, 1318–1323. https://doi.org/10.1111/jace.14108.
- Ti, R.; Lu, X.; He, J.; Huang, F.; Wu, H.; Mei, F.; Zhou, M.; Li, Y.; Xu, T.; Zhu, J. Multiferroic Properties and Magnetoelectric Coupling in Fe/Co Co-Doped Bi_{3.25}La_{0.75}Ti₃ O₁₂ Ceramics. *J. Mater. Chem. C Mater.* **2015**, 3, 11868–11873. https://doi.org/10.1039/C5TC02399H.
- 40. Komogortsev, S.V.; Iskhakov, R.S. Law of Approach to Magnetic Saturation in Nanocrystalline and Amorphous Ferromagnets with Improved Transition Behavior between Power-Law Regimes. J. Magn. Magn. Mater. 2017, 440, 213–216. https://doi.org/10.1016/j.jmmm.2016.12.145.
- Devi, E.C.; Soibam, I. Law of Approach to Saturation in Mn–Zn Ferrite Nanoparticles. *J. Supercond. Nov. Magn.* **2019**, 32, 1293–1298. https://doi.org/10.1007/s10948-018-4823-4.
- Yu, Z.; Meng, X.; Zheng, Z.; Lu, Y.; Chen, H.; Huang, C.; Sun, H.; Liang, K.; Ma, Z.; Qi, Y.; et al. Room Temperature Multiferroic Properties of Rare-Earth-Substituted Aurivillius Phase Bi₅Ti₃Fe _{0.7}Co_{0.3}O₁₅ Ceramics. *Mater. Res. Bull.* 2019, 115, 235–241. https://doi.org/10.1016/j.materresbull.2019.04.002.

Disclaimer/Publisher's Note: The statements, opinions and data contained in all publications are solely those of the individual author(s) and contributor(s) and not of MDPI and/or the editor(s). MDPI and/or the editor(s) disclaim responsibility for any injury to people or property resulting from any ideas, methods, instructions or products referred to in the content.